Bollettino di Geofisica Teorica ed Applicata Vol. 58, n. 4, pp. 285-302; December 2017
DOI 10.4430/bgta0203

Kinematic constraints of the active northern Matese Fault System (southern Italy)

A. Galderisi[1], P. Galli[2,3], S. Mazzoli[4] and E. Peronace[3]

[1] *Freelance geologist, Castel San Giorgio (SA), Italy*
[2] *Dipartimento della Protezione Civile, Roma, Italy*
[3] *CNR, Istituto di Geologia Ambientale e Geoingegneria, Roma, Italy*
[4] *Dipartimento di Scienze della Terra, dell'Ambiente e delle Risorse (DiSTAR), Università Federico II, Napoli, Italy*

(Received: April 3, 2017; accepted: July 31, 2017)

ABSTRACT Here we applied structural geology methodologies with the aim of unraveling the Quaternary history of the active northern Matese fault. This structure bounds the northern slopes of the Matese massif (Bojano basin), i.e., one of the most seismically hazardous regions of Europe which is the epicentral area of some of the strongest Italian earthquakes ($M_w \geq 6.6$). We focused on the northern Matese fault in order to investigate its Quaternary evolution, identifying the different kinematic phases from the end of the Pliocene to the Present. To achieve this goal we have applied a method of analysis correlating the structural information with geological, seismological and paleoseismological data. In particular, structural data provided the opportunity to derive the synthetic focal mechanisms that were successfully compared with the seismic focal mechanisms available for the area. Then, we determined Mohr-Coulomb circles in order to identify and distinguish the kinematic phases of optimally oriented fault development from those of later fault reactivation within a varied stress field. By integrating the results gathered from the structural analysis with available constraints provided by previous active tectonics studies, it was possible to reconstruct an evolutionary model for the main segment of the northern Matese fault during the Quaternary.

Key words: structural geology, fault kinematics, seismogenic fault, Matese massif, southern Apennines.

1. Introduction

Since the early studies on the active faults of the Italian Apennines (e.g., Bosi, 1975), investigators mainly focused on geomorphological, chronostratigraphic and, in some instances, paleoseismological analyses aimed at defining the seismogenic characteristics of the studied structure, such as the slip rate, the return time and the past, strong associated earthquakes. Little attention has usually been paid on the structural elements recorded by the carbonate slickensides, which, in turn, may account for the kinematic history of the fault through time, especially in relation with the past and the present stress fields. Indeed, as the Apennines are a fold-and-thrust-belt structure resulting from the latest stages of Miocene-Pliocene shortening in the Alpine-

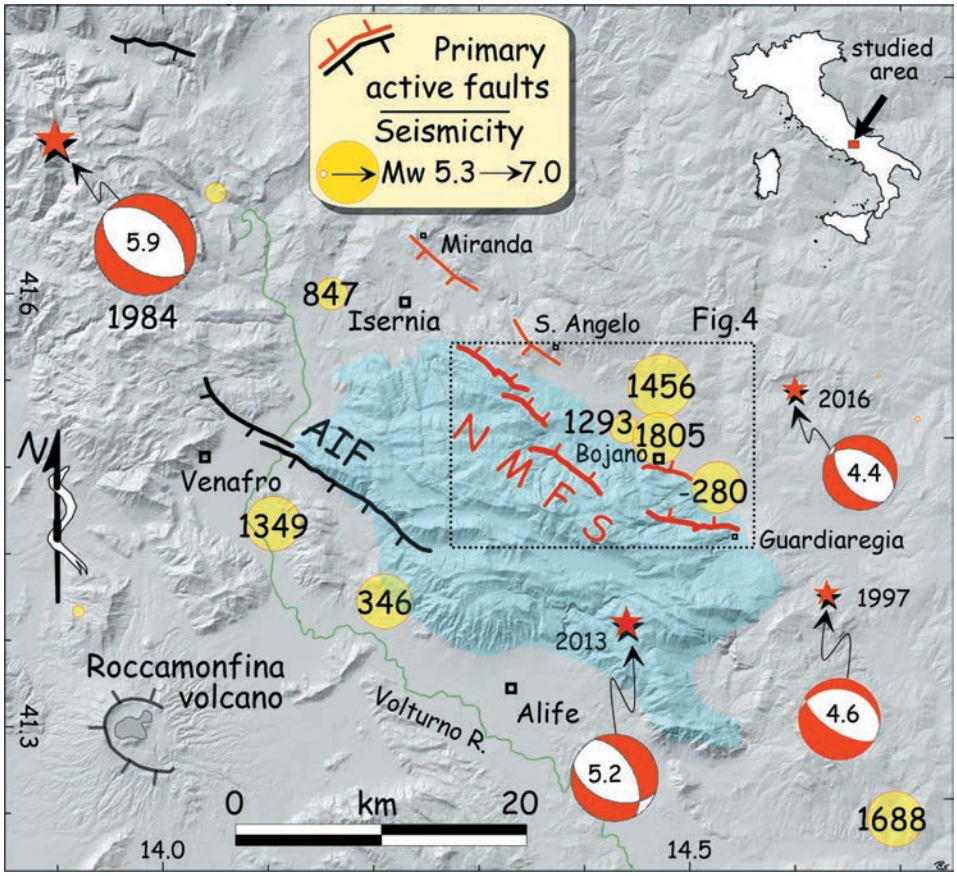

Fig. 1 - Index map of the investigated area (modified from Galli and Naso, 2009). Blue area: Matese massif; northern Matese Fault System (NMFS); Aquae Iuliae Fault (AIF). Yellow circles: main earthquakes of the region; focal mechanisms from RCMT (2016).

Mediterranean region, the presently active and seismogenic faults affecting the chain can be either newly-formed or inherited structural features that were re-activated as normal, oblique, or strike-slip faults since Middle Pleistocene times (~0.7 Ma; Dramis, 1992; Cinque *et al.*, 1993; Ascione *et al.*, 2013).

In this study, we apply an extensive geo-structural approach along the fault segments outcropping on the northern slopes of the Matese carbonate massif (Molise region, southern Italy: Fig. 1) aimed at recognizing the kinematic phases that characterized the fault system through time. The analyzed fault segments are part of the so-called northern Matese Fault System (NMFS; Galli and Galadini, 2003), which is considered one of the most hazardous structure of the whole Apennines. NMFS is a 28-km-long structure made by a complex right-stepping normal fault system bounding the Bojano Quaternary Basin. According to geological, geomorphological, geophysical, ^{14}C and tephrochronological analyses (Galli *et al.*, 2017), the NMFS had a slip rate > 1 mm/yr since the early-mid Middle Pleistocene, whereas both archaeoseismological and paleoseismological analyses revealed the occurrence of four $M_w > 6.6$ earthquakes in the past 3 ka (Galli *et al.*, 2017), three of which match the little known 280 BC event (Galli *et al.*, 2002, 2003), and the devastating 1456 (~M_w 7.0) and 1805 (M_w 6.6) earthquakes (Rovida *et al.*, 2016).

Our geo-structural survey was carried out all along the entire NMFS, and resulted in the measuring of about 900 fault elements (i.e., fault strike, dip, and different generations of kinematic indicators). The statistical analyses performed through the multiple inversion method (Yamaji, 2010) of such a huge number of data allowed us to reconstruct the strain and stress fields acting in the area today and in the past, together with the elaboration of synthetic focal mechanisms and Mohr-Coulomb circles. The cross-matching between all these results allowed to define the different kinematic phases of the NMFS during the whole Pleistocene.

2. Geologic and seismotectonic background

The Matese carbonate massif is mainly composed of shelf carbonates (D'Argenio *et al*., 1972), with a Meso-Cenozoic paleogeography controlled by high-angle normal faults. During the Neogene overthrusting of the Apennines units, these faults were tilted and offset by the basal detachment (Calabrò *et al*., 2003) that transported the carbonates to the east, over a footwall unit composed of basin deposits (Molise Unit). These thrust sheets were eventually emplaced on top of the Apulia Platform carbonates (Mostardini and Merlini, 1986; Patacca and Scandone, 2007). During the Pleistocene, extension was mainly accommodated by NW-SE striking normal faults, which also inverted favorably oriented structures inherited from the Neogene compressive phase (Ferranti, 1997), as well as by Pliocene-Early Pleistocene, ~E-W striking, high-angle transpressive faults, later mainly reactivated as dextral, transtensive splays. More in detail, according to Caiazzo (2000) and Cinque *et al*. (2000), during the Quaternary the southern Apennines were affected by two main, perpendicular extensional events. The older one, characterized by a NW-SE trending, horizontal maximum extension, lasted from the Early to the Middle Pleistocene, whereas the younger one is currently ongoing with a NE-SW trending, horizontal maximum extension. The first event generated NE-SW striking normal faults, and led to the reactivation of E-W and NW-SE striking faults with oblique-slip kinematics characterized by left-lateral components of motion accompanying the dip-slip extensional ones (Hippoliyte, 1992; Cinque *et al*., 2000; Caiazzo *et al*., 2006). On the other hand, the faults working during the younger (NE-SW) extensional phase were also preexisting NW-SE and E-W structures, that reactivated with an oblique-slip kinematics characterized by right-lateral components of motion (Caiazzo *et al*., 2006). Today, the faults bounding the massif toward the Bojano Plain make the NMFS (Galli and Galadini, 2003).

The Bojano alluvial plain hides below a semi-graben basin, with a master fault system outcropping to the south and an antithetic system buried to the north (e.g., Mazzoli *et al*., 2000). The detailed stratigraphy and the Middle-Late Pleistocene age of the fluvial-marshy and lacustrine-palustrine infilling have been constrained by Amato *et al*. (2014, 2016) and Galli *et al*. (2017) on the basis of both borehole analyses and field investigations, and through radiometric dating of tephra. Other Quaternary deposits mantle the slopes of the Matese Massif (Fig. 2), being both remnant of ancient fluvial-lacustrine units, and carbonate breccias sourced by the carbonate slopes during all the Pleistocene (Blumetti *et al*., 2000; Galli *et al*., 2002, 2017). Amongst the former, it is worth considering the lacustrine deposits described by Brancaccio *et al*. (1979) which contain tephra levels dated 582 ± 1 ka through $^{40}Ar/^{39}Ar$ method (Galli *et al*., 2017), while breccias has been analogously dated at 482 ± 3 ka.

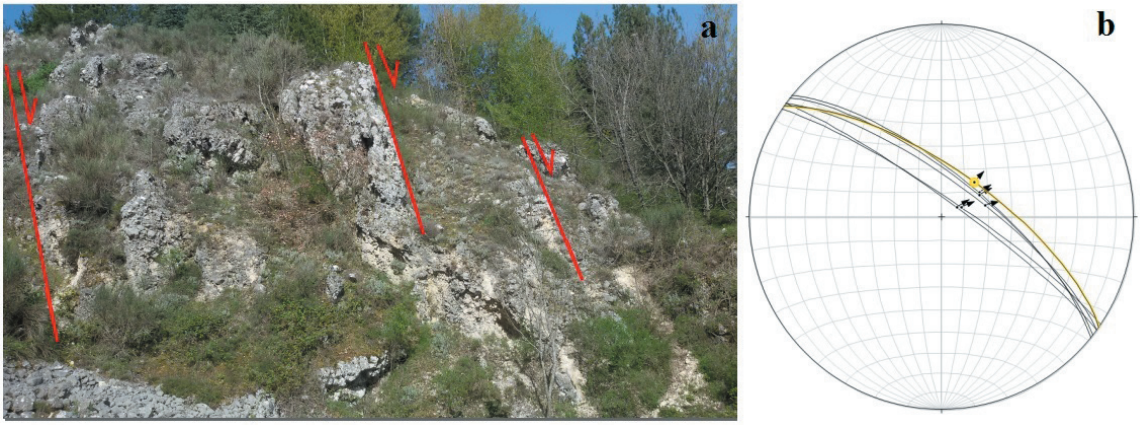

Fig. 2 - a) Cretaceous limestones (left) faulted against Middle Pleistocene breccias (middle-right) along the northernmost fault of the NMFS (Mount Patalecchia segment). Breccias are also affected by further splays and faulted against recent slope deposits (right). b) Stereogram of the secondary splays measured within the Pleistocene breccias, strictly matching a synthetic fault (in yellow) averaging all the data collected on the master fault of Mount Patalecchia.

As far as the Quaternary activity of the NMFS is concerned, it is worth summarizing here some indications suggested by different authors in the past. Blumetti *et al*. (2000) documented the offset of Holocene alluvial deposits inside a paleoseismic trench that was dug across the northernmost segment of the NMFS. In turn, Galli and Galadini (2003) provided evidence for a recent surface rupture along the southernmost segment. Moreover, besides the faulting of a last glacial maximum (LGM) alluvial fan, they also investigated the oblique right offset of the *temenos*-wall and the buildings of the Hercules' Italic temple affected by the fault. As a result of their study, Galli *et al*. (2017) confirmed the historical activity of the NMFS with new paleoseismic trenches and field observation carried out also along the intermediate fault segments, providing also a comprehensive framework of the Middle-Late Pleistocene tectonic evolution of the Bojano basin and of the latest associated destructive earthquakes.

Indeed, the region surrounding the Matese massif was struck by catastrophic earthquakes [$I_o \geq$ IX MCS, Mercalli-Cancani-Sieberg scale: see Sieberg (1930)] on record during the whole historical period (Rovida *et al*., 2016). The northern sector, i.e., that affected by the NMFS, has been the mesoseismic area of several high-magnitude events. In September 1293, Bojano was hit by an earthquake (M_w 5.8, I_o VIII - IX MCS) that killed many inhabitants, destroying castles and villages facing the plain (Castelli, 1993). Then, starting from December 5, 1456, the southern Apennines were struck by one of the most devastating sequence ever occurred in Italy (30,000 - 60,000 casualties), with at least three different epicentral areas, one (~M_w 7.0) matching with the Bojano basin (Magri and Molin, 1984; Meletti *et al*., 1988). Here, dozens of villages were razed to the ground (I_s X - XI MCS) killing several thousand people. A twin event occurred again in the Bojano basin less than four century later, when in July 26, 1805 a M_w 6.6 caused 5000 deaths, inducing site intensities of X MCS in those villages already hit in 1456 (Esposito *et al*., 1987). Last but not least, there is another strong event on record in the Bojano area which was discovered through archaeo-paleoseismic analyses in the Hercules' sanctuary of Campochiaro (easternmost segment of the NMFS in Fig. 1). Here Galli *et al*. (2002) dated the surface faulting of the sanctuary area to the early 3rd century B.C. (i.e., ~280 B.C.), relating this fact to an unknown earthquake.

As far as the indication of possible surface faulting, none of the historical primary sources of the 1456 earthquake report conclusive indication of ground breaks, either here or anywhere in the whole mesoseismic areas. In turn, many authors who described the 1805 effects provided reliable information concerning the opening of long chasms along the path of both the primary and antithetic splays of the NMFS (D'Onofrio, 1805; Duca della Torre, 1805; Fortini, 1805; Pepe, 1806; Poli, 1806), and particularly along the eastern segments.

In January 2016 (Milano, 2016) as in January 2017, two seismic swarms affected the investigated area (INGV, 2017). Two hundred events, with an M_L between 1.0 and 4.3, occurred in the hanging wall of the NMFS (depths mainly between 6-13 km), with a M_W 4.4 main shock sourced by a NW-SE normal fault (see the focal mechanism in Fig. 1).

2.1. The north Matese Fault System

The NMFS is made by several fault segments bounding the NE side of the carbonate Matese massif and by buried synthetic and antithetic faults. Recent studies (Galli *et al.*, 2017) evaluated the slip rates of these fault segments since the Middle Pleistocene, providing new clues on the seismogenic behavior and the interplay of each fault through time. The currently buried faults were likely the main structures that drove the early phase of the Bojano basin opening, transferring later the tectonic activity to the piedmont faults. Here we focused on the five main fault segments that run along the NE slope of the Matese massif for ~28 km (Fig. 1). These faults (Fig. 3) are all characterized by rock fault scarps and slickensides, presenting robust evidence of recent movements, such as faulting and tilting of post Late Pleistocene deposits (Galli *et al.*, 2017).

Fig. 3 - a) Late Pleistocene slope deposits progressively piled up and tilted against the Colle della Defenza fault (left). The yellow star indicates the sampling point of a trachytic tephra analyzed in Galli *et al.* (2017), and related to the Campanian Ignimbrite [40 ka according to Giaccio *et al.* (2017)]. b) Stereogram of fault planes belonging to the master fault of Campochiaro, recognized at the contact between carbonates and the Late Pleistocene slope deposits.

Slickensides are often dozen metres high, with an average strike of N320°, and a dip of 57° (Mount Patalecchia and Miletto slopes), and N270°, dip 50° (Campochiaro - Colle della Defenza slope, see Fig. 3).

3. Methodologies and analysis

3.1. Field investigations

A field survey (at the 1:10,000 scale) was conducted along the entire north-eastern slopes of the Matese massif, namely, from north to south: Mount Patalecchia (1400 m a.s.l.), Mount Miletto (2050 m a.s.l.) and Colle della Defenza (1220 m a.s.l.), for a length of about 28 km, focusing mainly along the NE-dipping slickensides. In order to determine fault kinematics, we performed a detailed structural survey by measuring strike and dip of the fault plane, abrasion *striae* and shear fibers, defined by rake, and shear sense obtained by calcite shear fibers steps and further, well-established kinematic indicators from brittle fault zones (e.g., Ramsay and Lisle, 2000, and references therein). In order to perform a representative statistical analysis of the NMFS, we gathered about 200 fault data from each segment, particularly focusing on complex areas. On each single fault plane, we paid attention in identifying overlapping relationships between different sets of *striae*/shear fibers, when present, in order to define the last slip phase and reveal the existence of previous episodes of deformation under different stress fields. Moreover, with the aim of determining the chronology of tectonic events, we verified the presence of further fault systems cross-cutting the NMFS. The identification of crosscutting relationships between faults and the definition of a hierarchy amongst *striae*/shear fibers sets are essential for the reconstruction of the evolution of fault systems.

3.2. Geo-structural analysis

Fault attitude and slip data were processed through the software FaultKin 5.2 (Allmendinger *et al.*, 2012). According to the theory of Anderson (1951), by defining the angle of internal friction between the fault plane and the P-axis $\theta = 30°$, we calculated the P and T-axes starting from the trend and the plunge of the *striae*/shear fibers. Moreover, by applying the principle of the Right Dihedra Method (Angelier and Mechler, 1977) on fault slip data, we derived the synthetic focal mechanisms for the individual fault segments. Hence, after subdividing the data of the various sets of *striae* following the field observations, we have reconstructed the paleo-synthetic focal mechanisms, that in turn is representative of the paleostress fields. Paleostress analysis provides the orientations of the three principal stress axes (σ_1, σ_2, and σ_3, with $\sigma_1 \geq \sigma_2 \geq \sigma_3$) and the stress ratio $R = (\sigma_2-\sigma_3) / (\sigma_1-\sigma_3)$ (Angelier, 1979). We have also applied an approach with the Mohr-Coulomb circles, aimed at identifying the phases of primary genesis and of subsequent fault reactivation within a different stress field, consistent with the principles of Coulomb fault development and Byerlee's law of frictional sliding (Byerlee, 1978; Ramsay and Lisle, 2000; Viola, 2008). In order to obtain information on the paleostress fields characterizing the study area, the Multiple Inversion Method (MIM: Yamaji, 2000) has also been applied. The MIM allows the separation of heterogeneous stress fields from fault-slip data. Heterogeneity is effectively taken into account by the applied method, which assumes that stresses with common principal orientations and common stress ratio represent a given state of stress. For areas such as those under investigation, which experienced various deformation stages associated with different stress states, it is reasonable to

assume that a group of faults was activated by an older stress state and another one by a younger stress state. In this instance, fault-slip data from all measured faults are defined as heterogeneous. In contrast, data from one fault group only is assumed to be homogeneous, and, therefore, bear information on the stress state corresponding to that specific group of faults. A heterogeneous data set may also be obtained from a rock mass in which the state of stress changed spatially and/or temporally. For a homogeneous data set, it is relatively easy to define the stress field associated with faulting by means of the classical stress inversion method (Angelier, 1979). The multiple inverse method aims at separating stresses numerically from heterogeneous data. For a homogeneous data set, the method provides not only the optimal solution, but also its confidence level. In order to analyze the temporal and/or spatial changes in the state of stress from a fault-slip data set, one should always take into account a possible heterogeneity of the data set. The MIM uses the classical scheme of stress tensor inversion (Angelier, 1979) that minimizes the sum of misfit angles between observed and calculated slip directions, the unique assumption being represented by the Wallace-Bott hypothesis (Wallace, 1951; Bott, 1959) for which the slip is parallel to the resolved shear stress. By this method, a reduced stress tensor can be determined which represents the stress tensors having common principal orientations and a common Φ value. By definition the value of Φ, which is the relative magnitude of the principal stresses ($\Phi = \sigma_2-\sigma_3 / \sigma_1-\sigma_3$), ranges from 0 to 1. The two cases of $\Phi = 0$ and $\Phi = 1$ (axial stresses) represent the stress states $\sigma_1 > \sigma_2 = \sigma_3$ and $\sigma_1 = \sigma_2 > \sigma_3$, respectively. Starting from a fault-slip data set, orientations of the stress axes are estimated for subsets, obtained considering all the combinations of a *k* number of fault data. The method allows one to select handily the σ_1 and σ_3 stress solutions on stress plots and verify the quality of the solution by means of the evaluation of the misfit angles, i.e., the angles between the measured slip vector and those theoretically calculated according to the selected stress solution.

4. Data and results

We collected more than 900 structural data, distributed among 127 measurement stations (Table 1, Fig. 4). The NMFS is composed of five main segments that extend along the north-eastern side of the Matese. From north to south, these are: Mount Patalecchia fault (MPF), Colle di Mezzo fault (CMF), Roccamandolfi fault (RF), Bojano fault (BF) and Campochiaro *alias* Colle della Defenza (CDF). Here we have grouped these fault segments into two areas, according to the general azimuth trend of the fault planes.

The northern area includes the segments of the MPF, CDF and RF, whose fault planes show a general NE-SW strike, a NE dip and either pure dip-slip kinematics or oblique-slip kinematics characterized by a largely dominant dip-slip normal component. The southern area includes the fault segments of the BF and CDF, whose planes strike approximately E-W, dip northwards and display oblique-slip kinematics with marked, either left- or right-lateral components of motion accompanying the dip-slip extensional one.

4.1. Northern area

The northern area, which includes the Mount Patalecchia and Mount Miletto slopes, shows huge fault scarps carved into Cretaceous carbonate rock, with a typical NW, Apennines trend. The three

Table 1 - Mean attitude of fault planes, relevant kinematic indicators and parameters resulting from synthetic focal mechanisms for different tectonic events. MPF (Mount Patalecchia fault); CMF (Colle di Mezzo fault); RF (Roccamandolfi fault); BF (Bojano fault); CDF (Colle della Defenza fault). NE-SW indicates the NE-SW trending faults group.

Fault segment	No. Measures	Strike (°)	Slip (°)	Pitch (°)	Kinematics	Striae		T Axis		P Axis	
						Trend (°)	Plunge (°)	Trend (°)	Plunge (°)	Trend (°)	Plunge (°)
MPF	177	N 321	57	88	N	47	57	50	12	238	78
CMF	131	N 316	63	92	N	50	63	47	18	221	72
RF	164	N 325	65	87	N	48	65	53	20	241	70
BF	71	N 289	61	94	N	27	61	22	16	189	74
BF	55	N 294	66	119	N-Ndx	78	53	45	16	163	58
CDF	93	N 273	59	92	N	7	59	4	14	177	76
CDF	79	N 268	62	64	N-Nsx	312	53	339	13	222	63
CDF	87	N 271	68	126	N-Ndx	64	49	27	15	138	53
NE-SW	46	N 237	66	95	N	339	66	331	21	137	69

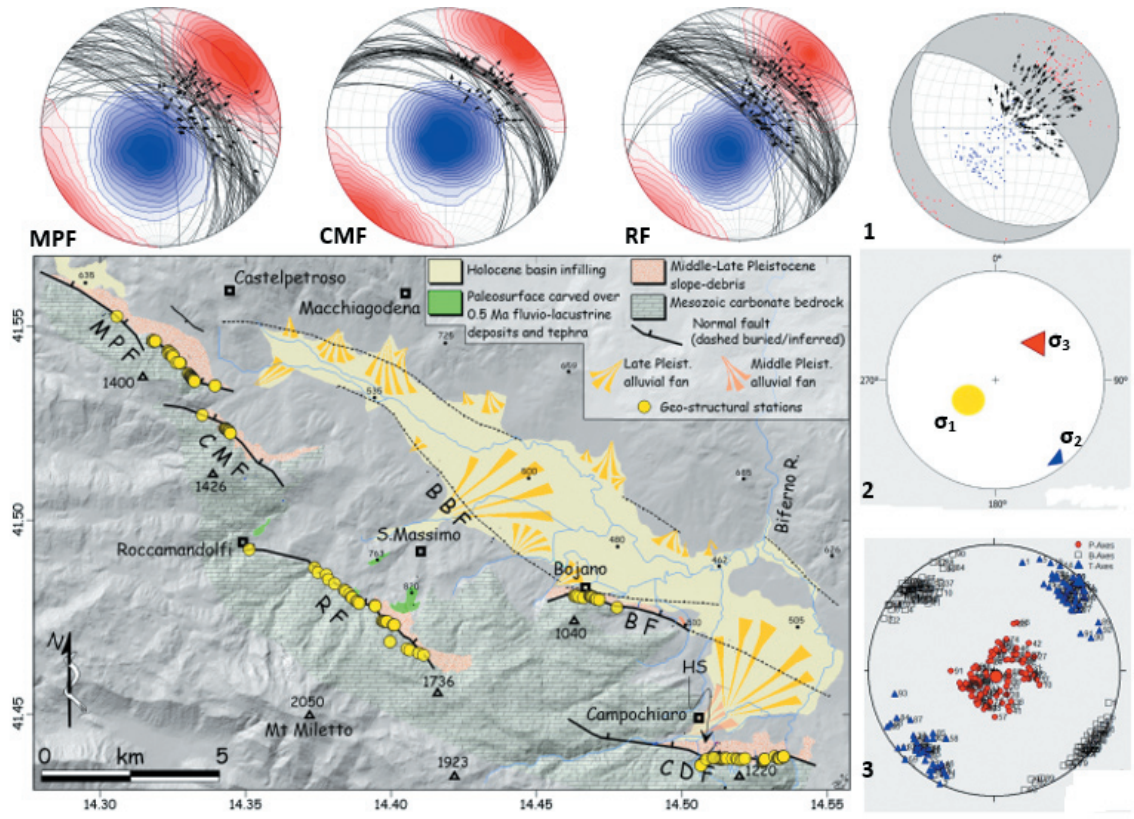

Fig. 4 - Digital Elevation Model of the Bojano basin area, with the path of the different segments composing the NMFS [MPF (Mount Patalecchia fault); CMF (Colle di Mezzo fault); RF (Roccamandolfi fault); BF (Bojano fault); CDF (Colle della Defenza)], and the main geological feature of the area. HS, Hercules' sanctuary. Yellow circles plotted along the faults represent the 127 geostructural stations. The three stereograms above show both the fault planes and the related *striae* trend (black arrows), besides the contouring of the P-axes (blue) and T-axes (red). 1) Cumulative synthetic focal mechanism of the fault segments of the northern sector. 2) Definition of the active stress field resulting from the inversion of the weighted average value of faults data. 3) Calculated field stress range through TectonicsFP software that indicates a direction of extension NE-SW, P-axis (red points), T-axis (blue triangles), B-axis (colorless square).

fault segments within this sector (MPF, CMF and RF in Fig. 4 and Table 1) are characterized by an average attitude of N320° and a dip of 58°. The field kinematic analysis carried out along the slickensides has allowed unraveling the relationships between the sets of *striae* and other kinematic indicators (Table 1). For instance, the calcite steps provide evidence for largely dominant normal-fault kinematics, matching the values of pitch angles that are within a range of 80°-105° (Fig. 4). The bending of the NMFS fault planes implies that as the strike of the slickenside deviates away from NW-SE, fault kinematics pass from almost pure dip-slip to more accentuated oblique-slip. In particular, the evidence of significant left-lateral components was observed on planes striking NNW-SSE, whereas right-lateral components occur on WNW-ESE striking, oblique-slip fault planes.

As the identification of the cross-cutting relationships between fault systems is fundamental for the understanding of the tectonic evolution of an area, we have carefully investigated this circumstance, finding that all the further, differently oriented faults were systematically cut by the NMFS (Table 1).

Fig. 5 - 1) High-angle slickenside outcropping along the MPF segment. 2) Fault plane along the CMF segment. 3) RF plane cutting a NE-SW fault.

One of the most widespread secondary systems systematically cut by the NMFS trends NE-SW. It has already been recognized both along the northern sector of eastern Matese and in other areas of the southern Apennines (e.g., Ferranti, 1997; Cinque *et al.*, 2000; Caiazzo *et al.*, 2006; Ferrarini *et al.*, 2017). Considering its hierarchical relationship with the NMFS, we can assess that the NMFS represents the latest active system in the region (Fig. 5).

4.2. Southern area

In the southern area, the NMFS affects the Bojano and Colle della Defenza slopes, with fault planes striking on average N272°, with a dip of 60° along the CDF, and N290°, dip 59° along the BF (Fig. 6 and Table 1). The structural data collected along these faults, and particularly along the CDF, show the occurrence of multiple sets of differently oriented *striae* and shear fibers. Indeed, it was possible to distinguish at least three sets of kinematic indicators on the same fault plane: a first one consists of *striae* with pitch angles ranging between 70° and 110° (i.e., 51% of

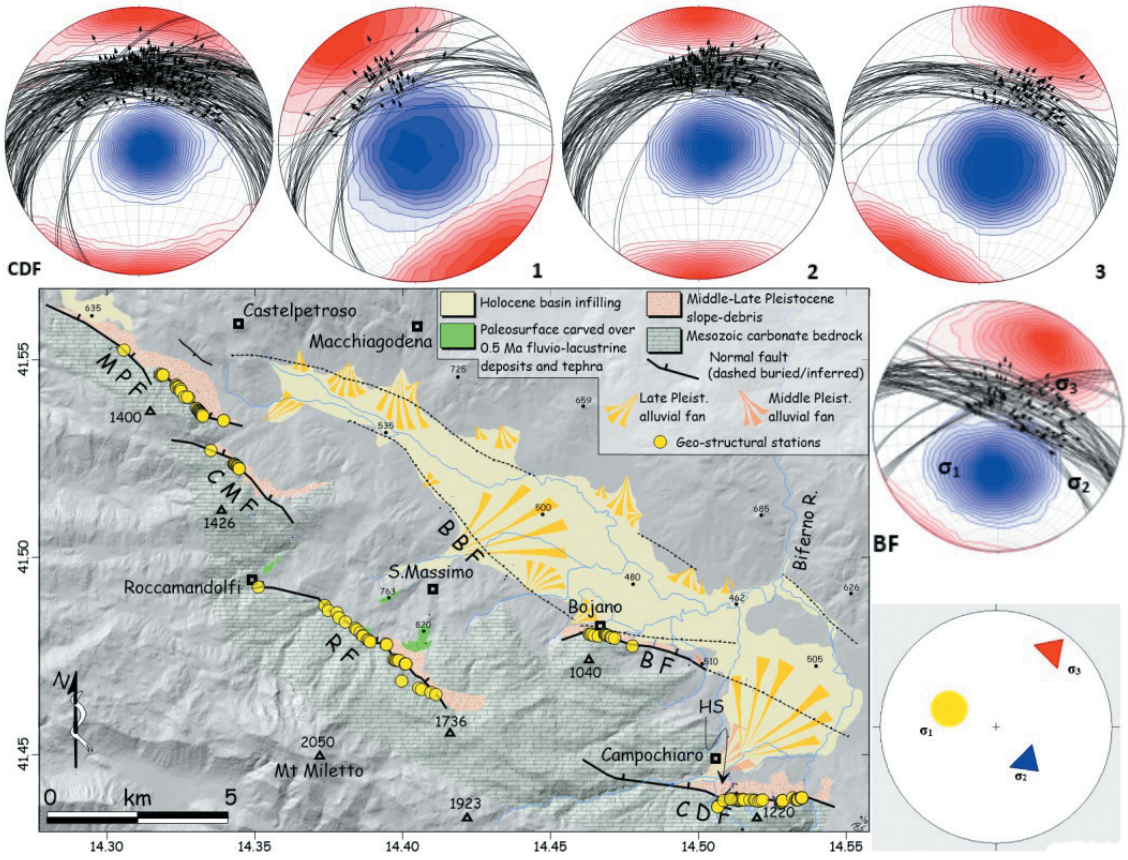

Fig. 6 - Digital Elevation Model of the Bojano basin area, with the same elements as in Fig. 4. Here stereograms account for data collected in the southern area, along the Boiano and Colle della Defenza faults. The CDF stereogram above shows the whole data set of fault planes and *striae* (black arrows), besides the contouring of the P-axes (blue) and T-axes (red). In turn, stereogram 1 accounts only for the dip-slip-dominated phase; stereogram 2 for the left-lateral oblique-slip; stereogram 3 for the right-lateral oblique-slip. BF stereogram (right) shows the whole data set of fault planes and *striae* (black arrows), besides the contouring of the P-axes (blue) and T-axes (red); stereogram 4 calculated field stress range by means of TectonicsFP software (from stereogram 3, right oblique-slip phase) that indicates a NE-SW direction of the maximum extension, P-axis (red points), T-axis (blue triangles), B-axis (colorless square).

Fig. 7 - 1) Slickenside in the carbonate rocks outcropping along the CDF. 2) Iron oxide on the fault plane highlighting a dextral oblique-slip kinematics. 3) Fault plane with different generation of striae indicating both right- and left-lateral, oblique-slip kinematics.

T-axes ranging between N340° and N20°), indicating oblique-slip kinematics largely dominated by a dip-slip component. A second one with values ranging between 40° to 70° (i.e., 29% of T-axes ranging between N20° and N40°), recording a significant left-lateral component of motion. A third one that partly overlaps the previous set, ranging from 110° to 140° (i.e., 21% of T-axes ranging between N300° and N340°), recording a substantial right-lateral component of motion (Fig. 7).

As the bending of the fault plane might generate *striae* with an apparent rake (e.g., Sippel *et al.*, 2009, 2010; Federico *et al.*, 2014), we adopted the multiple inversion method (Yamaji, 2010), avoiding thus errors in the statistical determination of the different kinematic phases. The three paleostress fields which resulted from this inversion match the three sets of *striae* observed on the fault planes (Fig. 7). The angular difference calculated on the weighted average value of σ3 axis of the dip-slip phase with respect to the oblique right-slip phase is of ~25°. In turn, the angular difference calculated on the weighted average value of σ3 axis of the dip-slip phase with respect to the oblique left-slip phase is of ~23°. These angular ranges match those commonly adopted in the

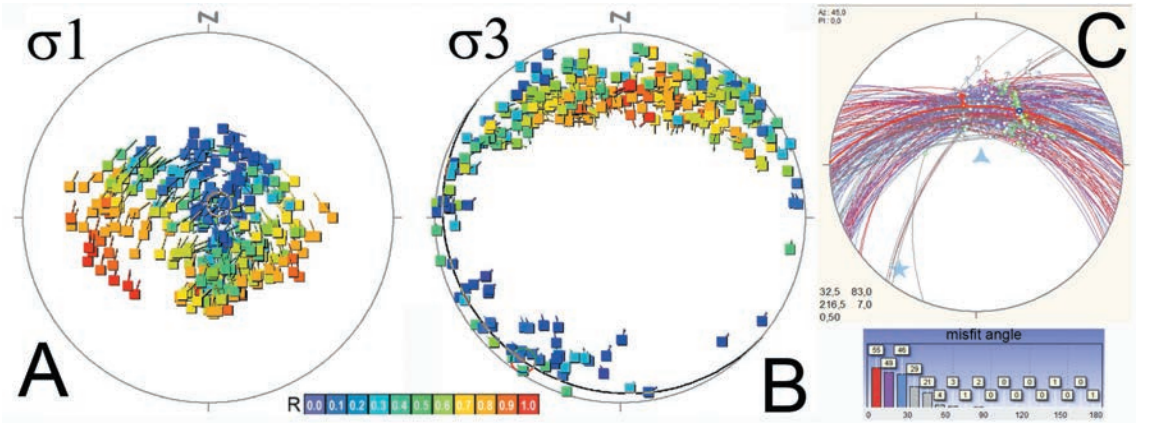

Fig. 8 - Colle della Defenza fault: example of use of program MIM (Yamaji, 2010) applied to the n = 212 fault-slip data (stereonet C) with a size of artificial subsets of $k = 4$. Each reduced stress tensor is plotted with its σ1-axis in the stereonet A and the associated σ3-axis in the stereonet B. The corresponding stress ratio, R = (σ2-σ3) / (σ1-σ3), is colour-coded. Mistfit angles between fault data and calculeted σ1-σ3 axis.

scientific literature (e.g., Wang and Neubauer, 1998; Lamarche *et al.*, 1999; Saintot and Angelier, 2002; Burg *et al.*, 2005; De Paola *et al.*, 2005; Lao-Davila and Anderson, 2009; Federico *et al.*, 2014). At the end, data presenting an angular difference between the oblique and dip-slip phases less than 5% were not taken into account as they could be hardly related to a specific kinematic phase. Considering the presence of these overlapping kinematic indicators, which were not so evident in the northern area, here we have applied an approach with the analysis of the Mohr-Coulomb circles. As previously mentioned, this analysis allows the identification of the newly generated fault planes vs those that were reactivated in subsequent phases, under a different stress field. By entering the fault data in the MIM software, we set a field of extensional stress and, applying Coulomb's failure criterion and Byerlee's law of stability of reactivation (Byerlee, 1978; Ramsay and Lisle, 2000; Viola, 2008), we unraveled different phases of fault genesis/reactivation (Fig. 8).

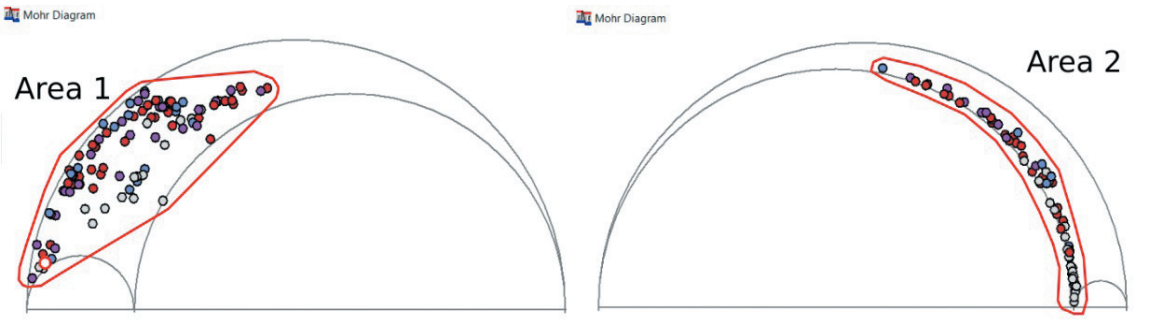

Fig. 9 - Left, Mohr-Coulomb diagram normalized for the dip-slip-dominated phases fault. The P-plane clustering in this area accounts for newly generated faults, compatible with the active extensional stress field (area 1). Right, Mohr-Coulomb diagram for the oblique-slip phases. The distribution of P-plane in this area is typical of reactivated fault, with P-plane not favorably oriented with respect to the extensional stress field (area 2).

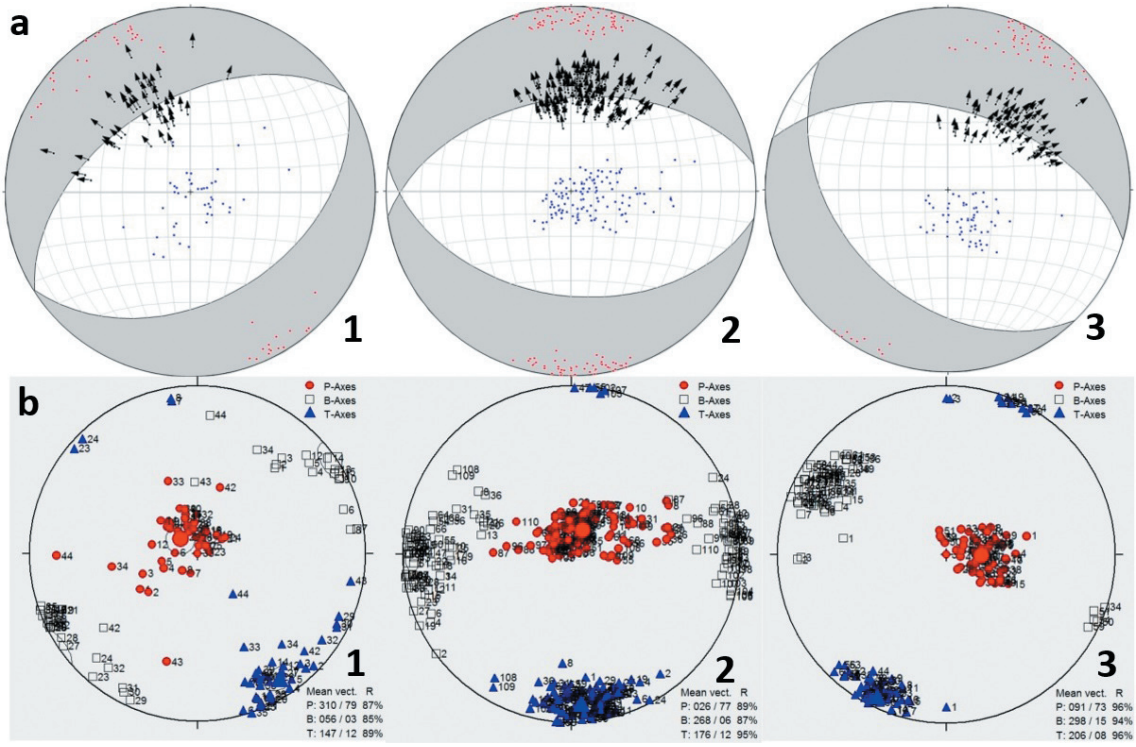

Fig. 10 - a) Synthetic focal mechanisms for the three kinematics phases recognized along the CDF (1: left-lateral oblique slip;2: dip-slip; 3: right-lateral oblique slip). Black arrows represent the striae trend; P-axis (blue points) and T-axes (red points). Note the full matching between the focal mechanism derived from the dextral oblique-slip phase and that calculated for the 2016 earthquake sequence (Fig. 1). b) Stress field and paleostress of CDF, resulting from the separation of the different kinematic phases. Note the three different directions of extension: NW-SE (1), N-S (2) and NE-SW (3).

By observing Fig. 9, it is evident that all the dip-slip data cluster in the area of tangency between the envelope curve and the Mohr circles (Area 1). Therefore, in agreement with Coulomb's failure criterion, this can be considered an evidence for the development of newly formed faults. On the other hand, the data with marked oblique-slip kinematics are distributed in an area where the Byerlee's law reactivation stability persists (Area 2). Therefore, this can be considered as an evidence for a phase of the reactivation of preexisting faults (Ramsay and Lisle, 2000; Viola, 2008).

The existence of various sets of kinematic indicators allowed us to produce synthetic focal mechanisms for the different kinematics phases (Fig. 10). For instance, it is worth noting that the CDF synthetic focal mechanism indicates oblique-slip kinematics with a dextral component of motion that fully matches the focal mechanisms calculated for the M_W 4.1 mainshock that occurred during the seismic sequence located in the CDF hanging wall in 2016 (Milano, 2016; Galli *et al*., 2017). We also carried out a similar analysis for the construction of the stress fields existing at the time of each kinematic stage. Indeed, once subdivided the data in the different kinematic phases, it was possible to determine the paleostress axes which led to the formation of the left-lateral oblique-slip kinematics phase (b2 in Fig. 10), that acting during the dip-slip phase (b1) and the most recent and still active (b3: right-lateral oblique slip).

5. Discussion and conclusions

On the basis of ~900 fault data collected during the field survey along the NMFS, we have carried out different kinds of statistical analysis that led to complementary geo-structural results. Joining these results with the field evidence concerning the activity of the NMFS through time (e.g., Galli *et al.*, 2017, and references therein) allowed us to provide new insights into the Quaternary evolution of this fault system.

One of the more important topics of this study has been the kinematic analysis of fault planes, and especially the identification of overlapping relationships among the different sets of *striae*. Firstly, we have investigated the latest kinematics indicators along the whole fault system. Older sets of kinematic indicators were also identified, allowing us to unravel different configurations of the stress field affecting the study area during previous deformation stages. The results of this study are used to provide a model of fault activity for the NMFS.

In the northern sector of the study area, we have systematically observed that fault planes striking ~N320° are characterized by *striae* consistently indicating pure dip-slip or oblique-slip kinematics largely dominated by dip-slip components of motion. On the other hand, faults striking ~N345° show younger, markedly oblique-slip kinematics characterized by significant left-lateral components of motion. Similarly, faults striking ~N300°, display younger oblique-slip kinematics characterized by substantial right-lateral components of motion (for instance, see MPF in Fig. 4).

In the southern sector of the study area, and especially along the mainly E-W trending CDF, we have observed that the *striae* set that always overlaps older ones is that indicating oblique-slip kinematics characterized by right-lateral components of motion. Therefore, assuming that these latest *striae* families indicate the main extensional direction, this implies that active faulting is driven by a NE-SW trending extension.

The data inversion method (e.g., Angelier, 1990) allowed us to infer the stress field acting on each segment of the fault system. The stress field deriving from the latest kinematic indicators (Figs. 4 and 6) matches the currently active stress over the central Apennines, characterized by a NE-SW trending maximum horizontal extension (e.g., Montone *et al.*, 2004; Serpelloni *et al.*, 2006; Palano *et al.*, 2011). By applying the Right Dihedra Method (Angelier and Mechler, 1977) to the collected fault data, we generated focal mechanisms that, at least for the latest phases of activity (Figs. 4, 9), fully match those evaluated for the 2016 local seismic sequence (RCMT, 2016 in Fig. 1).

In synthesis, it is possible to state that, in the northern sector, fault planes currently rupture in a dip-slip fashion, except those that do not strike NW-SE and that show oblique-slip kinematics. In turn, on the southernmost segments of the NMFS, the oblique-slip, right-lateral phase is that accommodating the current NE-SW maximum horizontal extension (Fig. 10A), as ultimately testified by the dextral-offset faulting of the Hercules' sanctuary wall of Campochiaro (Galli *et al.*, 2002). Besides this latest oblique-slip kinematics with a dextral component, the CDF clearly shows both a dip-slip and an oblique-slip, left-lateral movements (Fig. 10A, 1-2). These kinematics, which are often obliterated along the other segments of the fault system, account for previous paleostress fields. The analysis of the Mohr-Coulomb circles (Fig. 9) provides elements suggesting a normal fault, i.e., pure extensional dip-slip, genesis of the CDF, which was subsequently reactivated with an oblique-slip kinematics. Assuming that the CDF attitude

did not rotate during the Quaternary, it is possible to conclude that this fault, similarly to other E-W trending faults of the southern Apennines, was generated within a stress field dominated by a N-S trending maximum horizontal extension, as already proposed for the Late Pliocene by some authors (Cinque *et al*., 2000; Caiazzo *et al*., 2006). Moreover, it is likely that the younger *striae* set recorded along the CDF, recording oblique-slip with a left-lateral component, developed within a stressfield characterized by a NW-SE extension, as that recognized by Caiazzo *et al*. (2006) for the Early Pleistocene.

Thanks to its favorable orientation within the three aforementioned stress fields, this richness of *striae* generations on record over the slickenside of the CDF can be really compared to a palimpsest unraveling the kinematic history of this fault during the Quaternary. On the other hand, although the BF presents a right-lateral component that overlaps the dip-slip one, due to its N290° trend it was difficult to separate the two kinematic phases as we did for the CDF.

Summarizing the foregoing discussion, we can conclude that the analysis of the structural data collected all along the NMFS, coupled with the chronological and paleoseismological data recently published on this area (Galli *et al*., 2017), helped in depicting a reliable model of the fault activity throughout the Quaternary.

During the Late Pliocene, as a result of a paleo-stress field dominated by N-S crustal extension, E-W striking normal faults formed (or reactivated earlier structures of the fold and thrust belt), leaving their kinematic signatures through dip-slip, normal fault-related *striae*. In the Early Pleistocene, oblique-slip characterized by a left-lateral component of motion is recorded by *striae* on the same E-W faults, accounting for a different stress field dominated by NW-SE horizontal extension. Then, during the Middle Pleistocene, the onset of a new stress field oriented similarly to the present one drove the progressive opening of the Bojano basin along both a buried set of faults paralleling the southern border of the basin and successively along the NMFS (Galli *et al*., 2017). This is recorded by the faults (e.g., MPF) located in the northern sector of the study area, which display dominant normal fault-related, dip-slip *striae* along the newly formed NW-SE slickenside surfaces, and oblique-slip motion along NNW-SSE and ENE-WSW striking faults. In turn, faults in the southern sector (e.g., CDF) were reactivated during this youngest stage with an oblique-slip kinematics characterized by a right-lateral component of motion accompanying the dip-slip extensional one.

REFERENCES

Allmendinger R.W., Cardozo N. and Fisher D.; 2012: *Structural geology algorithms: vectors and tensors*. Cambridge University Press, Cambridge, UK, 302 pp.

Amato V., Aucelli P.P.C., Cesarano M., Jicha B., Lebreton V., Orain R., Pappone G., Petrosino P. and Russo Ermolli E.; 2014: *Quaternary evolution of the largest intermontane basin of the Molise Apennine (central-southern Italy)*. Rendiconti Lincei, **25**, 197-216.

Amato V., Aucelli P.P.C., Cesarano M., Cifelli F., Leone N., Mattei M., Russo Ermolli E., Petrosino P. and Rosskopf C.M.; 2016: The *infill timing of a quaternary intermontane basin: new chrono-stratigraphic and palaeoenvironmental data by a 900 m deep borehole fromCampochiaro (central-southern Apennine, Italy)*. In: Abstract, EGU General Assembly, Wien, Austria, Vol. 18.

Anderson E.M.; 1951: *The dynamics of faulting and Dyke formation with applications to Britain*. Oliver and Boyd, Edinburgh, UK, 191 pp.

Angelier J.; 1979: *Determination of the mean principal directions of stresses for a given fault population*. Tectonophys., **56**, T17-T26.

Angelier J.; 1990: *Inversion of field data in fault tectonics to obtain the regional stress - 111. A new rapid direct inversion method by analytical means*. Geophys. J. Int., **103**, 363-376.

Angelier J. and Mechler P.; 1977: *Sur une methode graphique de recherche des contraintes principales egalement utilisables en tectonique et en seismologie: la methode des diedres droits*. Bull. Soc. Géol. France, **19**, 1309-1318, doi:10.2113/gssgfbull.S7-XIX.6.1309.

Ascione A., Mazzoli S., Petrosino P. and Valente E.; 2013: *A decoupled kinematic model for active normal faults: insights from the 1980, M_S = 6.9 Irpinia earthquake, southern Italy*. Geol. Soc. Am. Bull., **125**, 1239-1259, doi:10.1130/B30814.1.

Blumetti A.M., Caciagli M., Di Bucci D., Guerrieri L., Michetti A.M. and Naso G.; 2000: *Evidenze di fagliazione superficiale olocenica nel bacino di Bojano (Molise)*. In: Extended Abstract, 19° Convegno Nazionale GNGTS , Roma, Italy, pp. 12-15.

Bosi C.; 1975: *Osservazioni preliminari su faglie probabilmente attive nell'Appennino centrale*. Boll. Soc. Geol. It., **94**, 827-859.

Bott M.H.P.; 1959: *The mechanics of oblique slip faulting*. Geol. Mag., **96**, 109-117.

Brancaccio L., Sgrosso I., Cinque A., Orsi G., Pece R. and Rolandi G.; 1979: *Lembi residui di sedimenti lacustri pleistocenici sospesi sul versante settentrionale del Matese, presso San Massimo*. Boll. Soc. Nat. Napoli, **88**, 275-286.

Burg J.-P., Celerier B., Chaudhry N.M., Ghazanfar M., Gnehm F. and Schnellmann M.; 2005: *Fault analysis and paleostress evolution in large strain regions: methodological and geological discussion of the southeastern Himalayan fold-and-thrust belt in Pakistan*. J. Asian Earth Sci., **24**, 445-467.

Byerlee J.D.; 1978: *Friction of rocks*. Pure Appl. Geophys., **116**, 615-629.

Caiazzo C.; 2000: *L'evoluzione tettonica del margine tirrenico dell'Appennino campanolucano; ricostruzione dei paleostress e analisi morfostrutturale*. Tesi di dottorato, Università di Napoli Federico II.

Caiazzo C., Ascione A. and Cinque A.; 2006: *Late Tertiary - Quaternary tectonics of the southern Apennines (Italy): new evidences from the Tyrrhenian slope*. Tectonophys., **421**, 23-51.

Calabrò R.A., Corrado S., Di Bucci D., Robustini P. and Tornagli M.; 2003: *Thin-skinned vs. thick-skinned tectonics in the Matese Massif, central-southern Apennines (Italy)*. Tectonophys., **377**, 269-297.

Castelli V.; 1993: *A cluster of earthquakes in the Apennines at the end of the XIII century*. Terra Nova, **5**, 496-502.

Cinque A., Patacca E., Scandone P. and Tozzi M.; 1993: *Quaternary kinematic evolution of the southern Apennines. Relationships between surface geological features and deep lithospheric structures*. Ann. Geofis., **36**, 249-260.

Cinque A., Ascione A. and Caiazzo C.; 2000: *Distribuzione spazio-temporale e caratterizzazione della fagliazione quaternaria in Appennino meridionale*. In: Galadini F., Meletti C. and Rebez A. (eds), Le ricerche del GNDT nel campo della pericolosità sismica (1996-1999), CNR-GNDT, Roma, Italy, pp. 203-218.

D'Argenio B., Pescatore T. and Scandone P.; 1972: *Schema geologico dell'Appennino meridionale (Campania e Lucania)*. In: Atti Convegno "Moderne vedute sulla geologia dell'Appennino", Accad. Naz. Lincei, **183**, 49-72.

De Paola N., Holdsworth R.E., McCaffrey K.J.W. and Barchi M.R.; 2005: *Partitioned transtension: an alternative to basin inversion models*. J. Struct. Geol., **27**, 607-625.

D'Onofrio A.; 1805: *Lettera ad un amico in provincia sul tremuoto accaduto a 2 luglio e seguito dall'eruzione vesuviana de 12 agosto del corrente 1805*. Napoli.

Dramis F.; 1992: *I1 ruolo dei sollevamenti ad ampio raggio nella genesi del rilievo appenninico*. Studi Geol. Camerti, Vol. Spec., **1**, 9-15.

Duca della Torre; 1805: *Notizie ricavate, ed osservazioni fatte in Contado di Molise, e precisamente in Bojano dopo il Tremuoto de' 26 di Luglio 1805*. Archivio comunale di Bojano.

Esposito E., Luongo G., Marturano A. and Porfido S.; 1987: *Il terremoto di S. Anna del 26 luglio 1805*. Mem. Soc. Geol. It., **37**, 171-191.

Federico L., Crispini L., Vigo A. and Capponi G.; 2014: *Unravelling polyphase brittle tectonics through multi-software fault-slip analysis: the case of the Voltri Unit, western Alps (Italy)*. J. Struct. Geol., **68**, 175-193.

Ferranti L.; 1997: *Tettonica tardo pliocenica - quaternaria dei Monti del Matese (Appennino meridionale): raccorciamenti e distensione "neotettonica"*. Il Quaternario (It. J. Quat. Sci.), **10**, 503-506.

Ferrarini F., Boncio P., De Nardis R., Pappone G., Cesarano M., Aucelli P.P.C. and Lavecchia G.; 2017: *Segmentation pattern and structural complexities in seismogenic extensional setting: the north Matese Fault System (central Italy)*. J. Struct. Geol., **95**, 93-112.

Fortini P.; 1805: *Delle cause de' terremoti e loro effetti*. In: Sardelli T. (ed), 1984, Danni di quelli sofferti dalla città d'Isernia fino a quello de' 26 luglio 1805, Marinelli, Isernia.

Galli P. and Galadini F.; 2003: *Disruptive earthquakes revealed by faulted archaeological relics in Samnium (Molise, southern Italy)*. Geophys. Res. Lett., **30**, 1266, doi:10.1029/2002GL016456.

Galli P. and Naso G.; 2009: *Unmasking the 1349 earthquake source (southern Italy). Paleoseismological and archaeoseismological indications from the Aquae Iuliae Fault*. J. Struct. Geol., 31, 128-149.

Galli P., Galadini F. and Capini, S.; 2002: *Analisi archeosismologiche nel santuario di Ercole di Campochiaro (Matese). Evidenze di un terremoto distruttivo sconosciuto ed implicazioni sismotettoniche*. It. J. Quat. Sci., **15**, 151-163.

Galli G., Giaccio B., Messina P., Peronace E., Amato V., Naso G., Nomade S., Pereira A., Piscitelli S., Bellanova J., Billi A., Blemart D., Galderisi A., Giocoli A., Stabile T. and Thil F.; 2017: *Middle to Late Pleistocene activity of the northern Matese Fault System (southern Apennines, Italy)*. Tectonophys., **699**, 61-81.

Giaccio B., Niespolo E., Pereira A., Nomade S., Renne P., Albert P., Arienzo I., Regattieri E., Wagner B., Zanchetta G., Gaeta M., Galli P., Mannella G., Peronace E., Sottili G., Florindo F., Leicher N., Marra F. and Tomlinson E.; 2017: *First integrated tephrochronological record for the last ~190 kyr from the Fucino Quaternary lacustrine succession, central Italy*. Quat. Sci. Rev., **158**, 211-234.

Hippoliyte J.C.; 1992: *Tecnonique de l'Apennin meridionale: structures et paleocontraintes d'un prisme d'accretion continentale*. PH.D. Thesis in Geological Sciences, Univ. de Paris 06, Paris, France, 338 pp.

INGV; 2017: *Italian Seismological Instrumental and parametric Data-base*. Istituto Nazionale di Geofisica e Vulcanologia,, Roma, Italy, <iside.rm.ingv.it/>.

Lamarche J., Mansy J.L., Bergerat F., Averbuch O., Hakenberg M., Lewandowski M., Stupnicka E., Swidrowska J., Wajspryc B. and Wieczorek J.; 1999: *Variscan tectonics in the Holy Cross Mountains (Poland) and the role of structural inheritance during Alpine tectonics*. Tectonophys., **313**, 171-186.

Lao-Davila D.A. and Anderson T.H.; 2009: *Kinematic analysis of serpentinite structures and the manifestation of transpression in southwestern Puerto Rico*. J. Struct. Geol., **31**, 1472-1489.

Magri G. and Molin D.; 1984: *Il terremoto del dicembre 1456 nell'Appennino centromeridionale*. Comitato Nazionale Energia Nucleare, Roma, Italy, 180 pp.

Mazzoli S., Corrado S., De Donatis S., Scrocca D., Butler R.W.H., Di Bucci D., Naso G., Nicolai C. and Zucconi V.; 2000: *Time and space variability of "thin-skinned" and "thick-skinned" thrust tectonics in the Apennines (Italy)*. Rend. Lincei, Sci. Fis. Nat., **11**, 5-39.

Meletti C., Patacca E., Scandone P. and Figliuolo B.; 1988: *Il terremoto del 1456 e la sua interpretazione nel quadro sismotettonico dell'Appennino meridionale*. In: Figliuolo B. (ed), Il Terremoto del 1456, Osservatorio Vesuviano e Istituto Italiano di Studi Filosofici, Storia e Scienze della Terra, Edizioni Studi Storici Meridionali, Altavilla Silentina (SA), **1**, 71-108, **2**, 35-163.

Milano G.; 2016: *Seismological investigation of the 2016 low magnitude seismic sequence near Baranello (Sannio-Matese area, southern Apennines - Italy): first results*. In: Extended abstract, 35° Convegno Nazionale GNGTS, Lecce, Italy, pp. 149-151.

Montone P., Mariucci M.T., Pondrelli S. and Amato A.; 2004: *An improved stress map for Italy and sourrounding region (central Mediterranean)*. J. Gephys. Res., **109**, B10410.

Mostardini F. and Merlini S.; 1986: *Appennino centro-meridionale. Sezioni geologiche e proposta di modello strutturale*. Mem. Soc. Geol. It., **35**, 177-202.

Palano M., Cannavò F., Ferranti L., Mattia M. and Mazzella M.E.; 2011: *Strain and stress fields in the southern Apennines (Italy) constrained by geodetic, seismological and borehole data*. Geophys. J. Int., **187**, 1270–1282, doi:10.1111/j.1365-246X.2011.05234.x.

Patacca E. and Scandone P.; 2007: *Geology of the southern Apennines*. Bull. Soc. Geol. It., Vol. Spec., **7**, 75-119.

Pepe G.; 1806: *Ragguaglio istorico-fisico del tremuoto accaduto nel Regno di Napoli la sera de' 26 luglio 1805*. Napoli, 172 pp.

Poli G.S.; 1806: *Memoria sul tremuoto de' 26 luglio del corrente anno*. Napoli.

Ramsay J.G. and Lisle R.J.; 2000: *Fault slip analysis and stress tensor calculations*. In: The Techniques of Modern Structural Geology, Volume 3: Applications of continuum mechanics in structural geology, Academic Press, San Diego, Session 32, pp. 785-810.

RCMT; 2016: *European-Mediterranean RCMT Catalog*. <www.bo.ingv.it/RCMT/>.

Rovida A., Locati M., Camassi R., Lolli B. and Gasperini P.; 2016: *CPTI15, the 2015 version of the Parametric Catalogue of Italian Earthquakes*. Istituto Nazionale di Geofisica e Vulcanologia, Roma, Italy, 33 pp., doi:10.6092/INGV.IT-CPTI15.

Saintot A. and Angelier J.; 2002: *Tectonic paleostress fields and structural evolution of the NW-Caucasus fold-and-thrust belt from Late Cretaceous to Quaternary*. Tectonophys., **357**, 1-31.

Serpelloni E., Anzidei M., Baldi P., Casula G., and Galvani A.; 2006: *GPS measurements of active strains across the Apennines (Italy)*. Ann. Geophys., **49**, 319– 332.

Sieberg A.; 1930: *Geologie der Erdbeben*. Handboch Geophys., **2**, 552-554.

Sippel J., Scheck-Wenderoth M., Reicherter K. and Mazur S.; 2009: *Paleostress states at the south-western margin of the central European Basin System e application of fault-slip analysis to unravel a polyphase deformation pattern*. Tectonophys., **470**, 129-146.

Sippel J., Saintot A., Heeremans M. and Scheck-Wenderoth M.; 2010: *Paleostress field reconstruction in the Oslo region*. Mar. Petrol. Geol., **27**, 682-708.

Viola G.; 2008: *Ductile and brittle structural evolution of the Laxemar-Simpevarp area: an independent analysis based on local and regional constraints*. Svensk Kärnbränslehantering AB, Stockholm, Sweden, Rapport R-08-124, 87 pp.

Wallace R.E.; 1951: *Geometry of shearing stress and relationship to faulting*. J. Geol., **59**, 111-130.

Wang X. and Neubauer F.; 1998: *Orogen-parallel strike-slip faults bordering metamorphic core complexes: the Salzach-Enns Fault Zone in the eastern Alps, Austria*. J. Struct. Geol., **20**, 799-818.

Yamaji A.; 2000: *The multiple inverse method: a new technique to separate stresses from heterogeneous fault-slip data*. J. Struct. Geol., **22**, 441-452.

Yamaji A. *et al.*; 2010: *Multiple inversion method software, Version 6.02*. Division of Earth and Planetary Sciences, Kyoto University.

Corresponding author: Antonio Galderisi
Via E. Lanzara 4, Castel San Giorgio (SA), Italy
Phone: +39 3927202820; e-mail: a.galderisi92@gmail.com